Proc. Natl. Acad. Sci. USA
Vol. 96, pp. 1915–1920, March 1999
Biochemistry

Native display of complete foreign protein domains on the surface of hepatitis B virus capsids

PETER A. KRATZ*, BETTINA BÖTTCHER†, AND MICHAEL NASSAL*‡

*University Hospital Freiburg, Department of Internal Medicine II/Molecular Biology, Hugstetter Strasse 55, D-79106 Freiburg, Germany; and †Institute of Physical Chemistry, University of Freiburg, Albertstrasse 23a, D-79104 Freiburg, Germany

Communicated by F. William Studier, Brookhaven National Laboratory, Upton, NY, December 30, 1998 (received for review November 2, 1998)

ABSTRACT **The nucleocapsid of hepatitis B virus (HBV), or HBcAg, is a highly symmetric structure formed by multiple dimers of a single core protein that contains potent T helper epitopes in its 183-aa sequence. Both factors make HBcAg an unusually strong immunogen and an attractive candidate as a carrier for foreign epitopes. The immunodominant c/e1 epitope on the capsid has been suggested as a superior location to convey high immunogenicity to a heterologous sequence. Because of its central position, however, any c/e1 insert disrupts the core protein's primary sequence; hence, only peptides, or rather small protein fragments seemed to be compatible with particle formation. According to recent structural data, the epitope is located at the tips of prominent surface spikes formed by the very stable dimer interfaces. We therefore reasoned that much larger inserts might be tolerated, provided the individual parts of a corresponding fusion protein could fold independently. Using the green fluorescent protein (GFP) as a model insert, we show that the chimeric protein efficiently forms fluorescent particles; hence, all of its structurally important parts must be properly folded. We also demonstrate that the GFP domains are surface-exposed and that the chimeric particles elicit a potent humoral response against native GFP. Hence, proteins of at least up to 238 aa can be natively displayed on the surface of HBV core particles. Such chimeras may not only be useful as vaccines but may also open the way for high resolution structural analyses of non-assembling proteins by electron microscopy.**

Hepatitis B virus (HBV), the causative agent of B-type hepatitis in humans (1), is a small enveloped DNA-containing virus that replicates via reverse transcription (2, 3). Its icosahedrally symmetric capsid, or core particle, is built from multiple subunits of a single 183-aa core protein (Fig. 1*A*), with the N-terminal 144 aa constituting the actual assembly domain (4, 5). During infection, the protein assembles around a complex of viral genomic RNA with the reverse transcriptase (6, 7). Inside the capsid, the RNA is reverse transcribed into partially double-stranded DNA. By budding into compartments of the secretory pathway, the capsids are exported as enveloped infectious virions.

Almost all HBV-infected individuals—even those that become chronic carriers—mount a strong, long-lasting humoral response against the capsid, or HBcAg, that is mainly directed against a single immunodominant epitope ("c") around amino acid 80. As its primary sequence overlaps with the e1 epitope of a nonassembling, antigenically distinct core protein variant known as HBeAg (8), the corresponding segment is referred to as the c/e1-epitope.

Crucial for the exceptional immunogenicity of HBcAg are the presence in its primary sequence of potent T helper epitopes and the high density of repetitively displayed structural features on the core particle (9) that explains its ability to also act as T cell-independent antigen (10, 11). Hence the HBcAg has gained interest as a carrier system to potentiate humoral as well as cellular immune responses against heterologous epitopes fused to the core protein (11, 12). Ideally, the foreign sequence should not affect particle formation and should be exposed on the particle surface. Empirical studies (13, 14) showed that the first criterion was met only by fusions to the termini of the core protein and the c/e1 epitope. The largest additions appeared to be tolerated at the C terminus; however, the added sequences were usually weakly immunogenic and the predominant response was directed against the authentic c/e1 epitope. Much better responses were obtained against insertions in the c/e1 epitope, yet the insert size compatible with particle formation appeared to be limited to around 50 (15), or in a single reported case, about 100 amino acids (16); furthermore, the spatial structure of none of the inserts has been determined.

Recent image reconstructions (17) from cryoelectron micrographs provided a structural basis for these observations (18, 19). They revealed two classes of core particles consisting of 120 and 90 dimeric subunits in T = 4 and T = 3 arrangements, in accord with the important role of the dimer indicated by previous biochemical data (20, 21). Each dimer forms a prominent spike on the particle surface. Electron density maps obtained at better than 10-Å resolution (22, 23) showed that the dimer interface consists of a four-helix bundle and led to a model for the main chain fold covering the N terminus to about position 140 (22). Further C-terminal residues would extend into the capsid interior, in accord with the internal localization of amino acid 150 (24). Biochemical interaction screens support this proposal by indicating the involvement of central residues in dimerization, whereas the interdimer contacts appear to be mediated by a network of C-terminal residues between positions 115 and 140 (25). Accordingly, each subunit provides to the dimer interface two long central α-helices (Fig. 1*B*). The short connecting loop comprises residues around P79 and hence largely overlaps with the c/e1 epitope that is most likely located at the tips of the spikes (26).

On this basis we reasoned that much larger inserts in the c/e1 site than previously thought might be tolerated, provided they would not interfere with formation of the major secondary-structure elements in the core protein's assembly domain. Accordingly, we prepared a DNA construct encoding a chimeric core protein in which amino acids P79 and A80 are replaced by the entire 238-aa green fluorescent protein (GFP) (Fig. 1 *C* and *D*) flanked by flexible linkers. Because both particle formation by the core protein and fluorophore generation by GFP depend on a native three-dimensional structure, production of fluorescent particles would indicate that the individual constituents of the chimeric protein are properly

The publication costs of this article were defrayed in part by page charge payment. This article must therefore be hereby marked "*advertisement*" in accordance with 18 U.S.C. §1734 solely to indicate this fact.

PNAS is available online at www.pnas.org.

Abbreviations: HBV, hepatitis B virus; HBcAg, hepatitis B core antigen; GFP, green fluorescent protein; CEM, cryoelectron microscopy.

‡To whom reprint requests should be addressed. e-mail: nassal2@ukl.uni-freiburg.de.

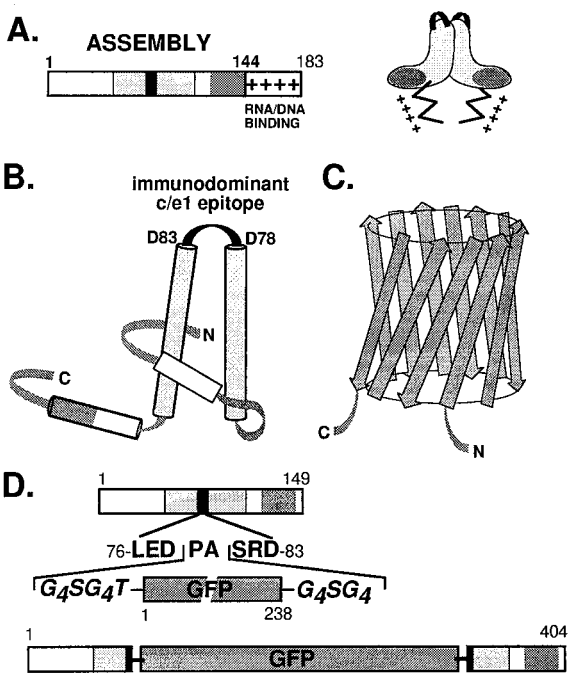

FIG. 1. Structural features of the constituent components of GFPcore1–149 (*A*) HBV core protein. The bar represents the primary sequence of the full-length core protein c1–183. Within the assembly domain (amino acids 1–144), the c/e1 epitope (black rectangle) and the regions involved in intradimer (light shading) and interdimer (dark shading) contacts are indicated. The Arg-rich nucleic acid binding domain is symbolized by +. A schematic topological view of the dimer is shown on the right. (*B*) Secondary structure model of the core protein. Cylinders represent α-helices, and the shading corresponds to that in *A*. The central helices are connected by a short loop overlapping with the c/e1 epitope. In the dimer, these helices form a four-helix bundle (adapted from ref. 22). N and C represent the N and C termini. (*C*) Schematic representation of GFP. The major secondary structure elements are β-strands forming an 11-stranded β-barrel (35, 36). (*D*) Chimeric GFPcore1–149 protein. The DNA construct was designed such that the entire GFP sequence, flanked on both sides by Gly-rich linkers, is inserted into the central c/e1 epitope of the truncated, assembly-competent core protein derivative core1–149; the authentic amino acids Pro-79 and Ala-80 are removed. The shading of core protein regions is as in *A*.

folded. As shown below, this is indeed the case. We also provide direct evidence for the surface exposure of the GFP domains and for the ability of these chimeric particles to evoke a strong humoral immune response against native GFP.

MATERIALS AND METHODS

Plasmid Constructs. The parental plasmid pPLC/c1–149 contains a synthetic gene (27) encoding the HBV core protein, subtype ayw (28), from amino acid 1 to 149 under control of the λ pL promoter (4). A new *Xho*I site was introduced by PCR-mutagenesis at nucleotide position 226 (TTGGAG $\rightarrow$ **CTC**GAG), giving plasmid pPLC/c1–149-Xho. A DNA insert encoding GFP flanked by Gly-rich linkers (Fig. 1*D*) was obtained by PCR with primers introducing terminal *Xho*I and *Xba*I sites using plasmid pTR-UF5 (29) as template; it encodes a fluorescence-enhanced GFP (eGFP) variant (Phe64Leu, Ser65Thr). This fragment was cloned into pPLCc1–149-Xho cut with *Xho*I and with *Xba*I at nucleotide position 241. The identity of the chimeric gene in the resulting plasmid pPLC/GFPc1–149 was confirmed by sequencing.

Expression and Partial Purification of GFPcore1–149 Protein. Plasmid pPLC/GFPc1–149 was transformed into *Escherichia coli* GI698 cells (Invitrogen), and expression was induced by addition of tryptophan (5) at 25°C for 16 h as described (25). Cells from a 0.5 liter culture were resuspended in 50 ml of PBS (pH 7.3) and lysed by sonication after adding 5.1 g of sucrose, 25 mg of lysozyme, 1 ml of 0.5 M EDTA and 5 ml of 10% Nonidet P-40. To the cleared lysate, ammonium sulfate was added to 40% saturation. The precipitate was suspended in 5 ml of PBS and dialyzed against 50 mM Tris·HCl, pH 7.5/100 mM NaCl buffer at 4°C. The cleared dialysate was loaded on a 60% to 10% (wt/vol) sucrose step gradient (2 ml each of 60%, 50%, 40%, 30%, and 20% and 0.5 ml of 10% sucrose) and centrifuged for 2 h at 41,000 RPM at 20°C in a TST41.14–41 rotor (Kontron, Zurich). Twelve fractions of 500 μl, eight fractions of 250 μl, and ten fractions of 500 μl were collected from the top to the bottom of the gradient. The total yield of chimeric protein was between 10 and 20 mg per liter of culture.

Protein Analysis. For SDS/PAGE anlysis (12.5% polyacrylamide; 0.1% SDS) the Laemmli system (30) was used; proteins were detected by Coomassie blue staining. Western blot analyses were performed as described (25), using primary antibodies against HBV core protein or GFP followed by appropriate secondary antibodies conjugated to peroxidase or alkaline phosphatase (Dianova, Hamburg, Germany) and the chemiluminescent substrates ECLplus (Amersham Pharmacia), or CDP-Star (Boehringer Mannheim). Bands were visualized using x-ray film or a DIANA charge-coupled device camera system (Raytest, Straubenhardt, Germany). Protein concentrations were determined by a Bradford assay (Bio-Rad), UV-VIS spectra were recorded on a Ultrospec 3000 photometer (Amersham Pharmacia).

Antibodies. For the detection of HBV core protein, the following antibodies were used: H800, a polyclonal rabbit antiserum raised against denatured recombinant c1–149 protein that reacts with all forms of core protein (4); mAbs 10E11 and 10F10, recognizing epitopes between amino acids 8 and 20 and 135 and 144 on denatured core protein (31); mAb mc312 directed against amino acids 78–83 and hence overlapping the c/e1 epitope (32). For GFP immunoprecipitation, a polyclonal rabbit antiserum (CLONTECH) was used, and for GFP detection on Western blots, a mixture of two mAbs (Boehringer Mannheim) was used.

Native Agarose Gel Electrophoresis. Aliquots from individual sucrose gradient fractions were loaded onto 0.8% (wt/vol) agarose gels in Bis/Tris/Pipes/EDTA (BTPE) buffer (33), pH 6.6, containing ethidium bromide (0.5 μg/ml) and were run at 5 V/cm. Nucleic acids and GFP proteins were visualized by illumination at 365 nm.

Immunization of Rabbits with GFPc1–149. For immunization, c1–149GFP protein was either used in native, particulate form with aluminum hydroxide or in denatured form after preparative SDS/PAGE with complete and subsequently, incomplete Freund's adjuvant to immunize rabbits at a commercial facility (Eurogentech, Brussels). The protocol involved four injections with 25 μg of each antigen (days 0, 14, 28, and 56).

Immunoprecipitation. Twenty microliters (gel bed) of protein A Sepharose (Amersham Pharmacia) loaded with 1 μl each of rabbit antisera against native GFPcore1–149 particles, denatured GFPcore1–149, or core1–149 (H800) and with 3 μg of polyclonal anti-GFP antibodies (CLONTECH) were incubated overnight with a mixture of about 1 μg each of GFPc1–149 and c1–149 capsids and purified eGFP (CLONTECH) in 200 μl of TNE buffer (10 mM Tris, pH 7.5/100 mM NaCl/0.1 mM EDTA) containing 3% BSA and 0.5% NP40. Bound proteins were released by boiling with sample buffer and after SDS/PAGE were analyzed by Western blotting using monoclonal anti-GFP antibodies or monoclonal anti-core antibody 10E11.

Electron Microscopy and Image Processing. For negative staining, appropriate sucrose gradient fractions were used

directly. For CEM, gradient-purified particles were dialyzed against PBS and concentrated to ≈5 mg/ml by using a Centricon 500 microconcentrator (Amicon). Samples for CEM were examined as described (18) by using a Philips EM 420 equipped with a Gatan cold stage. The temperature of the stage was maintained between 97 and 100 K. Micrographs were taken under low-dose conditions at a nominal magnification of ×60,000 with a 2-s exposure time. Suitable micrographs were scanned with a Zeiss SCAI scanner at a step size of 14 μm corresponding to 0.23 nm on the specimen. Image processing was carried out as described (22). As a starting point for the determination of the origins and orientations of the larger chimeric particles, a previously published map of T = 4 core shells was used (22). Each data set included about 1,000 particles.

RESULTS

Design of the Chimeric Core–GFP Expression Vector. GFP appeared to be an ideal model insert because its fluorescence depends on proper folding (34). In addition, both its N and C terminus are located at the same side of a rigid 11-stranded β-barrel structure (35, 36), an architecture (Fig. 1*C*) possibly facilitating the authentic interactions between the two separated halves of the core protein required to form an assembly-competent structure. To minimize steric constraints, Gly-rich linkers were added at both ends. An appropriate PCR fragment was inserted into a derivative of the expression vector pPLC/c1–149, which directs efficient production in *E. coli* of core protein c1–149 particles (4). The chimeric gene and its encoded protein, termed GFPcore1–149, are shown schematically in Fig. 1*D*.

Efficient Expression of Particulate GFPcore1–149 in *E. coli*. Expression of the chimeric gene in *E. coli* GI698 cells was induced as described (25). For a first characterization of the quaternary structure of the protein, cleared lysates were prepared that contained the bulk of fluorescent material. The protein fraction, precipitated with 40% saturated ammonium sulfate, was subjected to sedimentation in 10–60% sucrose gradients. Visible inspection showed two strongly fluorescent regions in the gradient, one slow- and one fast-sedimenting.

Individual gradient fractions were analyzed for total protein content by SDS/PAGE and Coomassie blue staining (Fig. 2*A*), which revealed an intense band at about 45 kDa in the top region (fractions 2–6) together with the bulk of *E. coli* proteins; a band of identical mobility was present in fractions 13–20 in significantly enriched form. The strength of these bands correlated with fluorescence intensity in the fractions. To confirm their identity, the same gradient fractions were analyzed by Western blotting using polyclonal anti-GFP antiserum and a monoclonal anti-core antibody, 10F10, recognizing an epitope outside the manipulated region. Both reacted with bands of identical mobility as the Coomassie-stained 45-kDa band (Fig. 2*B*).

As an independent test for particle formation, we used native agarose gel electrophoresis (37) in which ordered multisubunit particles [for instance, HBV capsids (4)] migrate as distinct sharp-edged bands through the gel. Because of their higher diffusion coefficients, nonassociating proteins appear as more diffuse bands. A corresponding analysis of the gradient fractions (Fig. 2*C*) revealed a faster and more diffuse fluorescent band in the upper fractions and a similarly strong fluorescent but sharper and slower migrating band in the lower fractions. This is particularly evident in a side-by-side comparison (Fig. 2*D*). This strongly suggested that the chimeric protein was able to form discrete particles. After blotting (25), both bands reacted with anti-GFP antibodies and a polyclonal anti-core antiserum but not with the monoclonal anti-core antibody mc312 (data not shown), in accord with disruption of its epitope by the GFP insert.

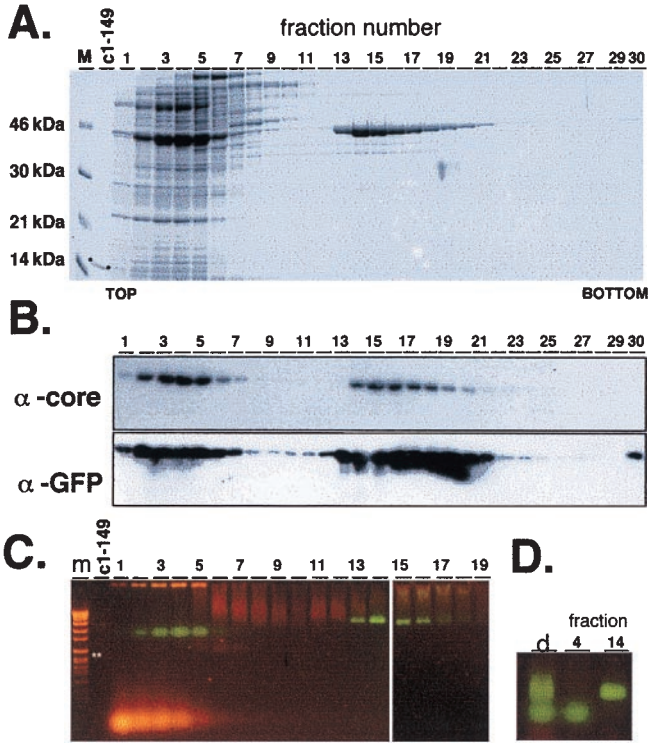

FIG. 2. Efficient synthesis of particulate GFPcore1–149 in *E. coli*. Cleared lysate from GFPcore1–149 expressing *E. coli* cells was subjected to sedimentation on a 10–60% sucrose gradient, and 30 fractions were collected from top to bottom. Aliquots of each fraction were analyzed by SDS/PAGE, Western blotting, and native agarose gel electrophoresis. (*A*) SDS/PAGE. The Coomassie blue-stained gel shows a prominent band of about 45 kDa in fractions 2–6 and a band of identical mobility in fractions 13–20. Both sets of fractions exhibited a strong green fluorescence. Apparent molecular masses of the marker proteins (lane M) are indicated at the left. c1–149 is a sample of authentic core protein 1–149 (∗). (*B*) Western blot. The presence of core-specific sequences in the 45-kDa protein was confirmed by using mAb 10F10 and that of GFP by using a commercial polyclonal anti-GFP antiserum. Bands were detected by chemiluminescence. (*C*) Native agarose gel electrophoresis. Aliquots from the gradient fractions were run alongside a DNA size marker (lane m) on gels containing ethidium bromide and visualized by illumination at 365 nm. A green fluorescent, more diffuse band is visible in fractions 2–6, a sharp-edged band of lower mobility in fractions 13–18. Orange bands result from ethidium bromide-stained nucleic acids. ∗ marks the position of authentic c1–149 capsids determined by subsequent Coomassie blue staining. (*D*) Direct mobility comparison of the fluorescent bands. Aliquots from unfractionated lysate (lane d) and from gradient fractions 4 and 14 were analyzed side-by-side.

At Least 40% of the Inserted GFP Domains Are Properly Folded. Native eGFP exhibits a strong absorbance in the visible range with a maximum at 488 nm and a molar extinction coefficient of $\varepsilon = 53{,}000\ M^{-1}\cdot cm^{-1}$ (38). For an estimate of the proportion of correctly folded GFP domains we measured the absorbance at 488 nm of aliquots from gradient fractions 14 to 16 (Fig. 2*A*) and correlated it with the protein concentrations determined by a Bradford assay. The GFP-specific maximum at 488 nm was clearly visible in the UV/VIS spectra, and the extinction coefficients calculated from the absorbances varied between ε = 22,000 and 26,600 $M^{-1}\cdot cm^{-1}$, i.e., between 42% and 50% of those expected if all GFP domains contained the authentic chromophore, if the protein was absolutely pure, and if close spacing between the GFP chromophores had no quenching effects. Hence, at least 40% of the GFP domains in the particulate chimeric protein are properly folded.

The Inserted GFP Domains Are Located on the Exterior of GFPcore1–149 Particles. To obtain direct information on the

structure of the *bona fide* chimeric particles, samples of the fast-sedimenting material were analyzed by CEM, which revealed abundant regular particles in two size classes, corresponding to the 180-subunit T = 3 and the 240-subunit T = 4 architectures (Fig. 3*A*). Their surface was distinctly rougher than that of particles from wild-type core protein, and for the T = 4 particles the diameter was increased from 33 nm (22) to about 40 nm. That these surface protrusions originate from GFP was confirmed by image reconstructions. Most of the extra density was present on the exterior of an otherwise wild-type-like inner shell (Fig. 3*B*); this is particularly evident from the equatorial cross section (Fig. 3*C*) revealing the typical T-shaped electron densities for some of the core protein dimers plus a more diffuse density surrounding the entire electron-dense inner shell. This similarity, together with the antigenicity and immunogenicity data presented below, strongly suggests that all GFP domains are presented on the surface of the chimeric particles. That the barrel structure of GFP does not become apparent is most likely caused by the flexible linkers that do not hold the GFP domains firmly in place.

Chimeric GFPcore Particles Effectively Elicit Antibodies Against Native GFP. To test the ability of the chimeric particles to induce antibodies against native GFP, rabbits were immunized with the purified particles, and for comparison with denatured antigen. A hallmark of HBcAg immunogenicity is the ability to elicit a potent response in the absence of strong adjuvants. Hence the native antigen was applied with aluminum hydroxide, a mild adjuvant approved for use in humans, whereas Freund's adjuvant was used with the denatured form. On Western blots developed with chemiluminescent substrates (Fig. 4*A*), both antisera, at a 1:100,000 dilution, detected 5 ng of the GFPcore1–149 protein, indicating efficient antibody induction by both antigens. However, only the serum against denatured antigen reacted with authentic core protein c1–149. A residual anti-core response was detectable with serum against native antigen when used at 10-fold higher concentration.

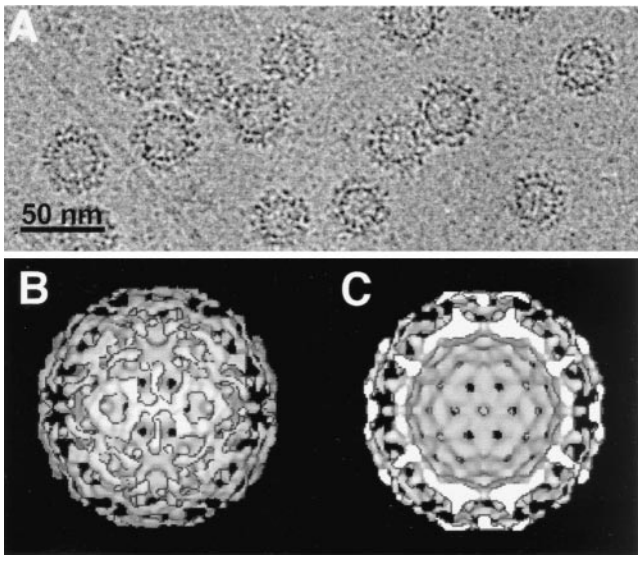

FIG. 3. Electron microscopy confirms the exterior location of GFP on chimeric GFPcore particles. (*A*) Cryoelectron micrograph. An aliquot from the particle fraction shows abundant particles in two size-classes. (*B* and *C*) Three-dimensional image reconstructions of the large (T = 4) GFPcore particles at 2-nm resolution. The surface view in *B* reveals a double-layered shell with the inner layer strongly resembling authentic core particles. The outer layer therefore most likely represents partially ordered GFP. The double-shell architecture is emphasized in the equatorial cross section in *C*. White areas correspond to high electron density.

Immunoprecipitation was used a more stringent test for the generation of antibodies against native GFP (Fig. 4*B*). A solution containing similar amounts of native eGFP, and of chimeric GFPcore and c1–149 particles was incubated with protein A Sepharose loaded with the rabbit sera against native and denatured GFPcore1–149; commercial purified polyclonal anti-GFP antibodies, and a polyclonal serum against core protein served as controls. Precipitated proteins were detected by Western blotting by using either monoclonal anti-GFP or anti-core antibodies (Fig. 4*B*). All antisera precipitated the GFPcore particles; precipitation by the anti-GFP antiserum independently confirmed the surface exposure of the GFP domains on the chimeric particles. However, a striking difference toward native GFP was observed: the serum against native GFPcore particles had precipitated even more GFP than the commercial anti-GFP antibodies (Fig. 4*B*, lane 1 vs. 3), whereas little if any GFP was brought down by the serum against denatured GFPcore1–149 (Fig. 4*B*, lane 2 vs. 3). This difference is even more obvious on a heavier exposure obtained after reprobing the anti-core blot with anti-GFP antibodies (Fig. 4*B*, lane 10 vs. 11). The anti-core blot (Fig. 4*B*, lanes 5 to 8) showed the strongest signal for core1–149 after immunoprecipitation with anti-core serum, followed by the serum against native and then denatured GFPcore1–149. The weaker reactivity of the latter antiserum compared with the direct Western blot (Fig. 4*A*) probably reflects that the majority of its anti-core antibodies are directed against epitopes not accessible on the intact particle. Together, these data demonstrate that the chimeric GFPcore particles are able to efficiently induce antibodies against native GFP and that the particulate structure is essential for this response.

DISCUSSION

The regular display of multiple identical structural features on the HBV core particle surface is crucial for its exceptional immunogenicity and ability to act as T cell independent antigen (9, 11, 39). Assembly competence and surface exposure are hence essential to provoke a strong response against a foreign sequence fused to the core protein. The c/e1 epitope has emerged as a superior insertion site with respect to the latter criterion (12). However, whereas small peptide inserts have long been known to be compatible with particle formation (27), its insertion capacity appeared to be limited (12) because any insert disrupts the primary sequence of the core protein and consequently affects its folding. Our study demonstrates that a complete foreign protein of about 240 aa can be displayed in multiple copies on the surface of chimeric HBV capsids. Remarkably, a large fraction of the foreign protein domains is present in a native state, and the chimeric particles efficiently induce antibodies against native epitopes of the protein graft without a strong adjuvant.

The biochemical evidence for the formation of ordered particles natively displaying GFP on their surface is based on the distinct sedimentation properties and, independently, the discrete appearance upon native agarose gel electrophoresis of the protein bands from the lower but not the top gradient fractions. As intended, the dependence of the GFP chromophore on a correct three-dimensional structure could be used to monitor folding of the chimeric GFPcore1–149 protein. Both the particulate and the slowly sedimenting fraction, probably consisting of unassembled dimers, exhibited a strong green fluorescence, i.e., both contained correctly folded GFP. Our estimate from the specific absorbance at 488 nm of at least 40% native GFP subunits on the particles bears several uncertainties, such as the unknown efficiency of chromophore formation, and a potential influence among the individual GFP chromophores by their close juxtaposition. Dimerization apparently reduces the long-wave absorbance of wild-type GFP to about one-fourth (40), and fluorescence resonance

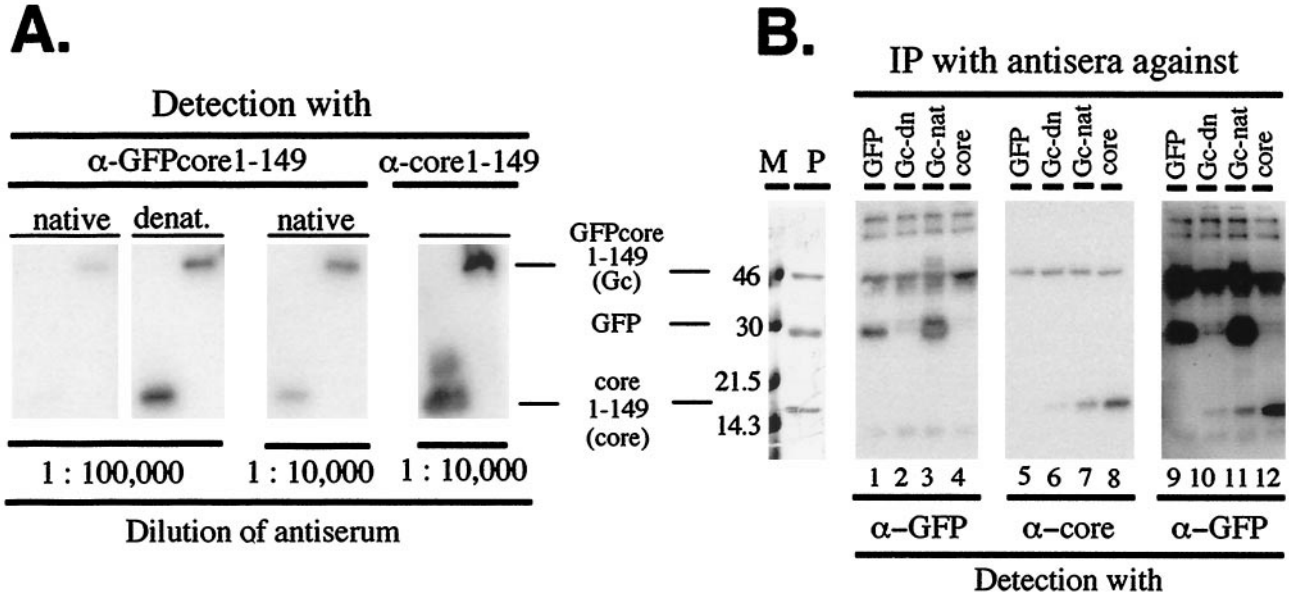

FIG. 4. Efficient antibody induction by GFPcore1–149. (*A*) Reactivity of anti-GFPcore1–149 antisera in Western blots. Poly(vinylidene difluoride) membranes containing GFPcore1–149 and core1–149 protein (5 ng per lane) were separately incubated with the rabbit antisera elicited against native particulate or denatured GFPcore1–149 protein at the indicated dilutions. A polyclonal serum against core1–149 protein served as control. Antigen-bound antibodies were visualized by using anti-rabbit-IgG-peroxidase conjugates and a chemiluminescent substrate. (*B*) Immunoprecipitation of native antigens by anti-GFPcore1–149 antisera. Native GFPcore1–149 (Gc) and core1–149 (core) particles and eGFP (GFP) were incubated with immobilized antibodies against native or denatured GFPcore1–149, against native GFP, and against core1–149 protein. Precipitated proteins were detected by Western blotting using monoclonal anti-GFP (lanes 1–4) or polyclonal anti-core antibodies (lanes 5–8) as in *A*. Lanes 9–12 show the anti-core blot after reprobing with anti-GFP antibodies. The left panel shows a Coomassie blue-stained SDS/PAGE gel of the input solution (lane P) alongside protein size markers (lane M). Note the efficient precipitation of native GFP by the serum against native (lanes 3 and 11) but not denatured (lanes 2 and 10) GFPcore1–149.

energy transfer can occur between different GFP variants if they are in close proximity (41). We therefore assume that the proportion of correctly folded GFP domains exceeds 50%, and may even be close to 100%.

Direct evidence for the formation of capsid-like particles with surface-exposed GFP domains was obtained by CEM and image reconstructions, revealing the presence of particles with the same T = 3 and T = 4 architectures as previously observed for authentic capsids (18, 19). The current data already establish a double-layered structure, of which the inner shell closely resembles authentic cores (22, 23); therefore, the outer density is contributed by GFP. At least a fraction of this density must be ordered and regularly arranged on the particle surface, otherwise it would not be visible. Surface exposure was independently confirmed by immunoprecipitation of the chimeric particles with GFP-specific antibodies and by their ability to elicit a strong anti-GFP response.

We envisage several reasons why, rather unexpectedly, substantially sized and natively folded inserts in the midst of the core protein sequence are tolerated. One is the intrinsically high stability of the entire assembly domain (42) and its individual secondary elements, in particular the long central helices. In this static view, the GFP insert may be regarded as a simple enlargement of the small connecting loop. However, a major problem that could account for previous problems is the potential occurrence of undesired interactions during folding (43) between the insert sequence and the split carrier moiety. In our case, the two regions of the core protein that must interact to form the assembly-competent structure are separated by more than 250 foreign residues. This requires that the individual core protein secondary structure elements can fold independently; hence, taking the sequence apart between two stable elements, such as the central helices, is probably essential. Similarly important is the ability of the insert to form a stable structure by itself. In this regard, a complete protein domain is more likely to behave as an independent folding entity than short fragments where unused contact sites would be available for side reactions leading to misfolding and/or aggregation. In addition, the connection between the insert domain and the two core protein subdomains must not sterically impair formation of the final structure. Likely, the flexible linkers at each end of the insert contributed to this requirement. Hence, we believe that the native display of other proteins (or protein domains) of the size of GFP and possibly larger can be accomplished. This view is supported by preliminary evidence suggesting that insertion of two unrelated 17-kDa proteins, the co-chaperone p23 and the duck homolog of interferon-γ, do not inhibit particle formation.

These results have several implications. Regarding the use of HBV cores as a vaccine carrier for natively displayed proteins, it is likely that similarly strong antibody responses as against GFP can be evoked against other native protein antigens. Whether all of the favorable properties of authentic HBcAg are maintained in chimeric particles whose surface is covered by heterologous protein remains to be determined. For instance, the direct T cell-independent activation of B cells (39) via surface Ig cross-linking, and the highly efficient uptake and presentation by B cells of HBcAg (9) appear to depend on an exact epitope spacing that could be altered in the chimeras. However, the principal requirement for repetitive epitope display is clearly fulfilled, and the presentation of a complete, native protein as opposed to a short peptide has its own advantages that could more than compensate such potential restrictions. For a peptide to be useful as a vaccine, the relevant epitopes have to be mapped beforehand, the structure of the peptide should mimic that in the natural context, and it should be presentable by the polymorphic major histocompatibility molecules of an outbred vaccinee population. All of these critical parameters have been difficult to translate into efficacious peptide vaccines (44). Most of them also pertain to capsid-like particles carrying a single heterologous epitope, although the problem of correct epitope conformation has

been successfully addressed by combinatorial libraries of linkers connecting a given peptide sequence in many different ways to human rhinovirus as a carrier (45, 46). They should be much less relevant, however, if a complete and natively folded foreign protein is displayed. Attractive candidates would be protein antigens from medically important microorganisms where evidence for a protective role of antibodies is available.

An intriguing perspective for structural studies is that proteins fused to the core particle framework, like the core protein itself, might become amenable to high-resolution EM analyses, and possibly x-ray crystallography, by exploiting the inherent noncrystallographic symmetry. Optimizing the flanking linker sequences should allow rigid fixing of the foreign protein domains to the surface such that they adopt topologically equivalent positions. Concerning specific applications of the GFPcore chimera, it might be used to follow the intracellular trafficking of authentic HBV core protein and also to trace the fate of capsid-like particles after administration into a complete organism.

We thank R. A. Crowther for making it possible to use the electron microscopy facility at the Laboratory of Molecular Biology, Medical Research Council, in Cambridge and V. Bichko and M. Noah for providing mAbs against HBV core protein. This work was supported by a grant from the Bundesministerium für Bildung und Forschung (BMBF-01KV9516) and by the Fonds der Chemischen Industrie.

1. Blumberg, B. S. (1997) *Proc. Natl. Acad. Sci. USA* **94,** 7121–7125.
2. Nassal, M. & Schaller, H. (1993) *Trends Microbiol.* **1,** 221–228.
3. Nassal, M. & Schaller, H. (1996) *J. Viral Hepat.* **3,** 217–226.
4. Birnbaum, F. & Nassal, M. (1990) *J. Virol.* **64,** 3319–3330.
5. Zlotnick, A., Cheng, N., Conway, J. F., Booy, F. P., Steven, A. C., Stahl, S. J. & Wingfield, P. T. (1996) *Biochemistry* **35,** 7412–7421.
6. Nassal, M. (1996) *Curr. Top. Microbiol. Immunol.* **214,** 297–337.
7. Seeger, C. & Hu, J. (1997) *Trends Microbiol.* **5,** 447–450.
8. Salfeld, J., Pfaff, E., Noah, M. & Schaller, H. (1989) *J. Virol.* **63,** 798–808.
9. Milich, D. R., Chen, M., Schödel, F., Peterson, D. L., Jones, J. E. & Hughes, J. L. (1997) *Proc. Natl. Acad. Sci. USA* **94,** 14648–14653.
10. Milich, D. R. & McLachlan, A. (1986) *Science* **234,** 1398–1401.
11. Milich, D. R., Peterson, D. L., Zheng, J., Hughes, J. L., Wirtz, R. & Schödel, F. (1995) *Ann. N.Y. Acad. Sci.* **754,** 187–201.
12. Ulrich, R., Nassal, M., Meisel, H. & Kruger, D. H. (1998) *Adv. Virus Res.* **50,** 141–182.
13. Schödel, F., Moriarty, A. M., Peterson, D. L., Zheng, J. A., Hughes, J. L., Will, H., Leturcq, D. J., McGee, J. S. & Milich, D. R. (1992) *J. Virol.* **66,** 106–114.
14. Schödel, F., Wirtz, R., Peterson, D., Hughes, J., Warren, R., Sadoff, J. & Milich, D. (1994) *J. Exp. Med.* **180,** 1037–1046.
15. Borisova, G., Borschukova Wanst, O., Mezule, G., Skrastina, D., Petrovskis, I., Dislers, A., Pumpens, P. & Grens, E. (1996) *Intervirology* **39,** 16–22.
16. Boulter, N. R., Glass, E. J., Knight, P. A., Bell-Sakyi, L., Brown, C. G. & Hall, R. (1995) *Vaccine* **13,** 1152–1160.
17. Mancini, E. J., de Haas, F. & Fuller, S. D. (1997) *Structure* **5,** 741–750.
18. Crowther, R. A., Kiselev, N. A., Böttcher, B., Berriman, J. A., Borisova, G. P., Ose, V. & Pumpens, P. (1994) *Cell* **77,** 943–950.
19. Kenney, J. M., von Bonsdorff, C. H., Nassal, M. & Fuller, S. D. (1995) *Structure* **3,** 1009–1019.
20. Zhou, S. & Standring, D. N. (1992) *Proc. Natl. Acad. Sci. USA* **89,** 10046–10050.
21. Nassal, M., Rieger, A. & Steinau, O. (1992) *J. Mol. Biol.* **225,** 1013–1025.
22. Böttcher, B., Wynne, S. A. & Crowther, R. A. (1997) *Nature (London)* **386,** 88–91.
23. Conway, J. F., Cheng, N., Zlotnick, A., Wingfield, P. T., Stahl, S. J. & Steven, A. C. (1997) *Nature (London)* **386,** 91–94.
24. Zlotnick, A., Cheng, N., Stahl, S. J., Conway, J. F., Steven, A. C. & Wingfield, P. T. (1997) *Proc. Natl. Acad. Sci. USA* **94,** 9556–9561.
25. König, S., Beterams, G. & Nassal, M. (1998) *J. Virol.* **72,** 4997–5005.
26. Conway, J. F., Cheng, N., Zlotnick, A., Stahl, S. J., Wingfield, P. T., Belnap, D. M., Kanngiesser, U., Noah, M. & Steven, A. C. (1998) *J. Mol. Biol.* **279,** 1111–1121.
27. Nassal, M. (1988) *Gene* **66,** 279–294.
28. Galibert, F., Mandart, E., Fitoussi, F., Tiollais, P. & Charnay, P. (1979) *Nature (London)* **281,** 646–650.
29. Zolotukhin, S., Potter, M., Hauswirth, W. W., Guy, J. & Muzyczka, N. (1996) *J. Virol.* **70,** 4646–4654.
30. Laemmli, U. K. (1970) *Nature (London)* **227,** 680–685.
31. Pushko, P., Sällberg, M., Borisova, G., Ruden, U., Bichko, V., Wahren, B., Pumpens, P. & Magnius, L. (1994) *Virology* **202,** 912–920.
32. Sällberg, M., Ruden, U., Magnius, L. O., Harthus, H. P., Noah, M. & Wahren, B. (1991) *J. Med. Virol.* **33,** 248–252.
33. Burnett, W. V. (1997) *BioTechniques* **22,** 668–671.
34. Niwa, H., Inouye, S., Hirano, T., Matsuno, T., Kojima, S., Kubota, M., Ohashi, M. & Tsuji, F. I. (1996) *Proc. Natl. Acad. Sci. USA* **93,** 13617–13622.
35. Ormö, M., Cubitt, A. B., Kallio, K., Gross, L. A., Tsien, R. Y. & Remington, S. J. (1996) *Science* **273,** 1392–1395.
36. Yang, F., Moss, L. G. & Phillips, G. N., Jr. (1996) *Nat. Biotechnol.* **14,** 1246–1251.
37. Serwer, P., Khan, S. A. & Griess, G. A. (1995) *J. Chromatogr.* **698,** 251–261.
38. Patterson, G. H., Knobel, S. M., Sharif, W. D., Kain, S. R. & Piston, D. W. (1997) *Biophys. J.* **73,** 2782–2790.
39. Fehr, T., Skrastina, D., Pumpens, P. & Zinkernagel, R. M. (1998) *Proc. Natl. Acad. Sci. USA* **95,** 9477–9481.
40. CLONTECH Laboratories, Inc. (1998) *Living Colors User Manual* (CLONTECH), p. 12.
41. Day, R. N. (1998) *Mol. Endocrinol.* **12,** 1410–1419.
42. Wingfield, P. T., Stahl, S. J., Williams, R. W. & Steven, A. C. (1995) *Biochemistry* **34,** 4919–4932.
43. Netzer, W. J. & Hartl, F. U. (1998) *Trends Biochem. Sci.* **23,** 68–73.
44. Rothbard, J. B. (1992) *Biotechnology* **20,** 451–465.
45. Arnold, G. F., Resnick, D. A., Smith, A. D., Geisler, S. C., Holmes, A. K. & Arnold, E. (1996) *Intervirology* **39,** 72–78.
46. Smith, A. D., Geisler, S. C., Chen, A. A., Resnick, D. A., Roy, B. M., Lewi, P. J., Arnold, E. & Arnold, G. F. (1998) *J. Virol.* **72,** 651–659.